

## ARTICLES

## Time-Resolved Absorption Studies on the Photochromic Process of 2H-Benzopyrans in the Picosecond to Submillisecond Time Domain

Yoichi Kodama,<sup>†,‡</sup> Takakazu Nakabayashi,<sup>‡</sup> Katsunori Segawa,<sup>†</sup> Emi Hattori,<sup>†</sup>  
Masako Sakuragi,<sup>§</sup> Nobuyuki Nishi,<sup>\*,‡</sup> and Hirochika Sakuragi<sup>\*,†</sup>

Department of Chemistry, University of Tsukuba, Tennodai, Tsukuba, 305-8571, Japan, Institute for Molecular Science, Myodaiji, Okazaki 444-8585, Japan, and National Institute of Materials and Chemical Research, Higashi, Tsukuba 305-8565, Japan

Received: June 5, 2000; In Final Form: August 17, 2000

Picosecond to submillisecond photochromic reactions of 2,4-diphenyl-2H-benzopyran and 2,2,4-triphenyl-2H-benzopyran have been investigated by time-resolved absorption spectroscopy. The C–O bond cleavage of the benzopyrans (closed forms) occurs via the first excited singlet state within 2 ps to produce vibrationally excited open forms in the ground electronic state. In the subnanosecond to submillisecond time domain, several decay components with almost the same spectral profiles are observed. These components are assigned to respective stereoisomers with respect to two double bonds and one single bond of the open enone forms. From the pump-laser power dependencies of the yields of the open forms, it is suggested that the photocleavage gives at first only the open forms revertible to the closed form by a single-bond rotation, and that the photoexcitation of the first generated open forms gives rise to other open forms which need a double-bond rotation for reversion to the closed form. The photochromic reactions of a series of 2H-benzopyrans bearing substituents on the pyran ring have also been studied using nanosecond time-resolved absorption spectroscopy. The size of a substituent in the 4-position fairly affects the rate constants of the thermal reversion of the open form to the closed form.

## 1. Introduction

Photochromic materials, which undergo light-induced transformation between two states exhibiting distinguishably different absorption spectra, have received great attention in recent years due to their potential applications in high-density optical storage and optical switching.<sup>1–4</sup> Among the most important classes of organic photochromic materials, spiropyrans and their analogues have been most extensively studied and best documented.<sup>1,2,5–19</sup> Spiropyrans consist of a pyran moiety and another moiety containing conjugated rings which are held orthogonal by a common spiro-carbon atom. The photochromic process in the spiropyran compounds features the dissociation of a C–O bond to produce a distribution of isomeric open forms (merocyanines), which are thermally and/or photochemically revertible to the original closed form. Extensive conjugation of the  $\pi$ -electron system in the open form leads to the appearance of the strong absorption in the visible region where the closed form does not absorb. The rate and mechanism of the reaction steps of some spiropyrans and their analogues have been examined with continuous absorption spectroscopy,<sup>15,17</sup> transient absorption spectroscopy,<sup>5,7,9–14,18,19</sup> and transient Raman spectroscopy.<sup>6,8,11,18,19</sup> Despite these efforts, the detailed dynamics of spiropyran

compounds have not been clarified because of the difficulties in assignment of the open forms involved. Their structural features arise from the heteroatoms included and the complicated molecular structure: (1) the open forms can take the ortho-quinoidal, zwitterionic, and hybrid structures,<sup>15</sup> and (2) the open forms can take stereoisomeric configurations with respect to the C=C double bonds.<sup>10</sup>

Since both the constituent  $\pi$ -electron systems do not interact significantly in the spiro form, the absorption spectrum of the spiropyran compound is approximately the superposition of the spectra of the two individual moieties. The C–O bond is cleaved by irradiation of UV light in the region where the pyran moiety absorbs. Furthermore, it is known that only 2H-benzopyrans (chromenes) and their analogues, which constitute the spiropyran compounds as the pyran moiety, also show photochromic behavior on UV irradiation.<sup>16,20–39</sup> From the absorption spectroscopy at low temperatures, Becker et al. have indicated that photoexcitation of the colorless benzopyran compounds proceeds through the C–O bond cleavage, resulting in a distribution of the colored open forms.<sup>20</sup> The generated open forms were shown to revert back to the original closed form either thermally or photochemically.<sup>20</sup> These results suggest that the photochromism of benzopyrans can be treated as the simplified model of that of spiropyrans. Some theoretical calculations have been carried out for the ring-opening reactions of 2H-benzopyrans,<sup>16,25,32</sup> in order to ultimately understand the photochromism of spiropyran. 2H-Benzopyran analogues have now been utilized as

\* Corresponding authors. E-mail: nishi@ims.ac.jp; sakuragi@staff.chem.tsukuba.ac.jp.

<sup>†</sup> University of Tsukuba.

<sup>‡</sup> Institute for Molecular Science.

<sup>§</sup> National Institute of Materials and Chemical Research.

**TABLE 1: Absorption Maxima of the Closed ( $\lambda_{\text{closed}}$ ) and Open Forms ( $\lambda_{\text{open}}$ ), Lifetimes ( $\tau_{\text{open}}$ ), Activation Energy ( $E_a$ ), and Frequency Factors ( $A$ ) for Disappearance of the Major Open Forms**

compound	R <sup>1</sup>	R <sup>2</sup>	R <sup>3</sup>	R <sup>4</sup>	R <sup>5</sup>	$\lambda_{\text{closed}}/\text{nm}$	$\lambda_{\text{open}}^a$		$\tau_{\text{open}}$	$E_a/\text{kJ mol}^{-1}$	$\log(A/\text{s}^{-1})$
							$\lambda_A/\text{nm}$	$\lambda_B/\text{nm}$			
BP	H	H	H	H	H	265 311		430	> 1 ms	nd <sup>b</sup>	nd
4-MeBP	H	H	Me	H	H	258 309		420	276 $\mu\text{s}$	41.2	10.8
4-PhBP	H	H	Ph	H	H	270 311		435	194 $\mu\text{s}$	40.7	10.9
2-PhBP	Ph	H	H	H	H	266 312	375 395	445	> 1 ms	nd	nd
4-Me-2-PhBP	Ph	H	Me	H	H	259 312	385 405	435	75.6 $\mu\text{s}$	35.8	10.4
2,4-Ph <sub>2</sub> BP	Ph	H	Ph	H	H	265 309	384 408	455	48 $\mu\text{s}$	34.3	10.3
2,2-Ph <sub>2</sub> BP	Ph	Ph	H	H	H	266 310	385 405	485	> 1 ms	nd	nd
4-Me-2,2-Ph <sub>2</sub> BP	Ph	Ph	Me	H	H	264 309		470	36 $\mu\text{s}$	33.6	10.3
2,2,4-Ph <sub>3</sub> BP	Ph	Ph	Ph	H	H	273 311		490	12 $\mu\text{s}$	28.9	10.0
2,2-Me <sub>2</sub> BP I	Me	Me	H	H	MeO	282 304		430	> 1 ms	nd	nd
2,2-Me <sub>2</sub> BP II	Me	Me	H	MeO	MeO	278 325		430	> 1 ms	nd	nd
2,2-Me <sub>2</sub> BP III	Me	Me	H	MeO	EtO	278 325		430	> 1 ms	nd	nd

<sup>a</sup>  $\lambda_A$  and  $\lambda_B$  are absorption maxima of A and B bands, respectively. <sup>b</sup> nd stands for "not determined".

ophthalmic glasses,<sup>33</sup> and their photochromic reactions have also been investigated for practical applications.<sup>28,31,33,38</sup>

Recently, Delbaere et al. have identified the structures of geometrical isomers involved in the photochromism of 3H-naphthopyrans with lifetimes in the second to minute range by means of UV and NMR spectroscopy.<sup>36</sup> However, very little is known about the time developments of 2H-benzopyrans and their analogues immediately after photoexcitation. Knowledge on the dynamics in all the time-region involved is essential for a detailed understanding of these photochromic reactions. In the present paper, we report on the time-resolved absorption study on the photoexcitation dynamics of 2,4-diphenyl-2H-benzopyran (2,4-Ph<sub>2</sub>BP) and 2,2,4-triphenyl-2H-benzopyran (2,2,4-Ph<sub>3</sub>BP) from picoseconds to submilliseconds. The dynamics of the ring-opening and the subsequent isomerization of the open forms are discussed on the basis of the results obtained. Nanosecond time-resolved absorption measurements on the dynamics for the thermal ring closure of a series of benzopyrans bearing substituents on the pyran ring are also made, to reveal structural factors controlling the dynamics of the thermal reversion of the open form to the closed form.

## 2. Experimental Section

**2.1. Materials.** 2H-Benzopyran (BP) and its derivatives employed in this study are listed in Table 1. All the compounds except methoxy derivatives were prepared as follows.

2H-Benzopyran<sup>40</sup> was prepared by dehydration of 4-chromanone.

4-Methyl-2H-benzopyran (4-MeBP)<sup>41</sup> and 4-methyl-2-phenyl-2H-benzopyran (4-Me-2-PhBP)<sup>41,42</sup> were prepared by dehydration of the products of the Grignard reactions of methyl iodide with 4-chromanone and flavanone, respectively.

4-Phenyl-2H-benzopyran (4-PhBP)<sup>40,41</sup> and 2,4-diphenyl-2H-benzopyran (2,4-Ph<sub>2</sub>BP)<sup>40,41</sup> were prepared by dehydration of the products of the Grignard reactions of bromobenzene with 4-chromanone and flavanone, respectively.

2,2-Diphenyl-4-methyl-2H-benzopyran (2,2-Ph<sub>2</sub>-4-MeBP) was prepared by dehydration of the product of the Grignard reaction of bromobenzene with 4-methylcoumarin,<sup>42</sup> which was prepared by a reaction of phenol and ethyl acetoacetate in nitrobenzene in the presence of aluminum chloride.<sup>43</sup>

2-Phenyl-2H-benzopyran (2-PhBP),<sup>44</sup> 2,2-diphenyl-2H-benzopyran (2,2-Ph<sub>2</sub>BP),<sup>44,45</sup> and 2,2,4-triphenyl-2H-benzopyran (2,2,4-Ph<sub>3</sub>BP)<sup>46</sup> were prepared by condensation of phenol with 1-phenyl-2-propyn-1-ol, 1,1-diphenyl-2-propyn-1-ol, and 1,1,3-triphenyl-2-propyn-1-ol, respectively.

7-Methoxy-2,2-dimethyl-2H-benzopyran (2,2-Me<sub>2</sub>BP I), 6,7-dimethoxy-2,2-dimethyl-2H-benzopyran (2,2-Me<sub>2</sub>BP II), and 7-ethoxy-6-methoxy-2,2-dimethyl-2H-benzopyran (2,2-Me<sub>2</sub>BP III) were commercially available from Aldrich. All experiments were carried out in cyclohexane under argon at room temperature (298 K). Sample solutions were prepared in concentrations of  $2 \times 10^{-4}$  mol dm<sup>-3</sup> in quartz cuvettes with 1 cm path length. Solvent cyclohexane (Dojin, Spectrograde) was used as received.

**2.2. Nanosecond Laser-Flash Photolyses.** Nanosecond laser-flash photolyses were performed using an excimer laser (Lambda Physik LPX-100, XeCl, 308 nm, 100 mJ/pulse, 20-ns) and a pulsed xenon arc (Ushio UXL-150, 150 W) as a monitoring light source. The monitoring beam obtained from the xenon lamp was oriented perpendicularly to the exciting laser beam, passed through a sample cell and a grating monochromator (JASCO CT-25C), and detected with a photomultiplier (Hamamatsu Photonics R928). The amplified signal was recorded as the time profile of a transmittance change on a storage oscilloscope (Iwatsu TS-8123), and accumulated for 3–5 times to be averaged. The system was computer-controlled and the decay curves were analyzed by this computer system.

**2.3. Picosecond Laser-Flash Photolyses.** A beam from a frequency-doubled cw mode-locked Nd:YAG laser (Coherent Antares 76S, wavelength 532 nm, repetition rate 76 MHz, average power 1.5 W, pulse duration 70 ps) was used to excite a dual jet hybridly mode-locked dye laser (Coherent 702-1). Light pulses with 590 nm wavelength, 3 ps duration, and 1 nJ pulse energy were obtained at a repetition rate of 76 MHz. The gain dye and saturable absorber used were Rhodamine 6G and DODCI, respectively. Pulses from the dye lasers passed through a dye amplifier (Quantel PTA-10) and amplified pulses with pulse energies of 0.8 mJ were obtained at a repetition rate of 10 Hz. The dye amplifiers were excited by the second harmonic of the output from a pulsed Nd:YAG regenerative amplifier (Quantel RGA60-10, 532 nm, 10 Hz, 200 mW, 70 ps) seeded by the cw mode-locked Nd:YAG laser. Kiton Red in water was used as the amplifying dye solution in this study.

The second-harmonic of the output from the dye amplifier was used as the pump beam (295 nm), and the remaining visible radiation was focused into a cell containing water to generate picosecond continuum. The generated continuum was passed through a blue glass filter to produce the probe light in the 390–500 nm region, and was split into two parts, one for a probe beam and the other for a reference. After passing through fixed (for the pump beam) and variable (for the probe beam) optical delay lines, the pump and probe beams were focused noncollinearly into the sample cell and the transmitted light intensities

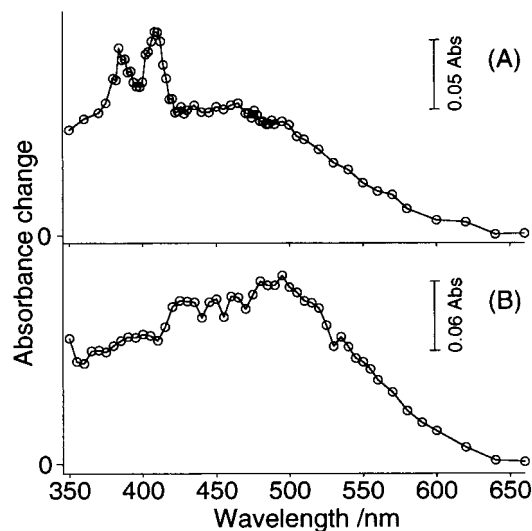


**Figure 1.** Nanosecond transient absorption spectra of (A) 2,4-Ph<sub>2</sub>BP and (B) 2,2,4-Ph<sub>3</sub>BP in cyclohexane excited at 308 nm. Delay time, (A) 185 and (B) 312 ns.

were detected by multichannel photodiodes (Hamamatsu Photonics C2326-22A) and collected at a 10 Hz repetition rate synchronized with the light source. The instrumental response function was determined by temporal rises of the excited-state absorption of *trans*-stilbene, 1,4-diphenylbutadiene, and naphthalene. It was estimated to be a Gaussian function with a full width at half-maximum of 4.5 ps.

For the measurements with the excitation at 266 nm, a regeneratively amplified output of Ti:sapphire laser was used as a light source. This laser system was based on a mode-locked Ti:sapphire laser (Spectra Physics Tsunami 3950, 800 nm, 82 MHz, 1.0 W, 3 ps) pumped by a CW argon ion laser (Spectra Physics BeamLok 2060). The oscillator was seeded into a regenerative amplifier (Spectra Physics TSA-10), which was pumped by the second harmonic output from a Q-switched Nd:YAG laser (Quanta-Ray GCR 150-10, 532 nm, 10 Hz, 1.5 W, 6–7 ns). The output pulses from the regenerative amplifier had 3 mJ pulse energy at a repetition rate of 10 Hz. The third-harmonic of the output from the regenerative amplifier was used as the pump beam, and the residual fundamental radiation was focused into a water-cell to generate picosecond continuum. The detection system was the same as described above.

### 3. Results

**3.1. Time-Resolved Absorption of Benzopyrans.** All the benzopyrans (closed form) used in this study exhibit two absorption bands around 270 and 310 nm as listed in Table 1. On UV excitation, these molecules exhibit absorption spectra in the visible region. Figure 1 shows nanosecond transient absorption spectra of 2,4-Ph<sub>2</sub>BP and 2,2,4-Ph<sub>3</sub>BP in cyclohexane solution. The spectrum from 2,4-Ph<sub>2</sub>BP exhibits a structured band with two sharp peaks around 400 nm (A band) and a broad band around 450 nm (B band), while that from 2,2,4-Ph<sub>3</sub>BP gives only the broad B band around 490 nm. The spectral and decay profiles are not affected in the presence of oxygen. The absence of any oxygen effects on the formation and the nanosecond-induced spectra of benzopyrans have already been reported together with the lack of any observable triplet states.<sup>26</sup> Therefore, the spectra in Figure 1 can be attributed to the ground-state open forms generated via the excited singlet states in comparison with the reported spectra for some benzopyrans.<sup>20–23,26</sup>

Figure 2A shows spectral changes in the delay time of 10–80 ps on excitation of 2,4-Ph<sub>2</sub>BP at 295 nm; a broad spectrum

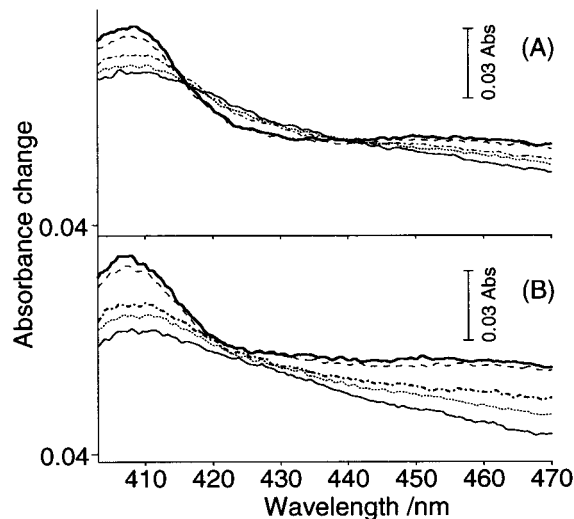


**Figure 2.** Picosecond time-resolved absorption spectra of 2,4-Ph<sub>2</sub>BP on the time scale from 10 to 80 ps excited at (A) 295 and (B) 266 nm. Thin solid line, 10 ps; dotted line, 15 ps; dash-dotted line, 20 ps; dashed line, 50 ps; thick solid line, 80 ps.

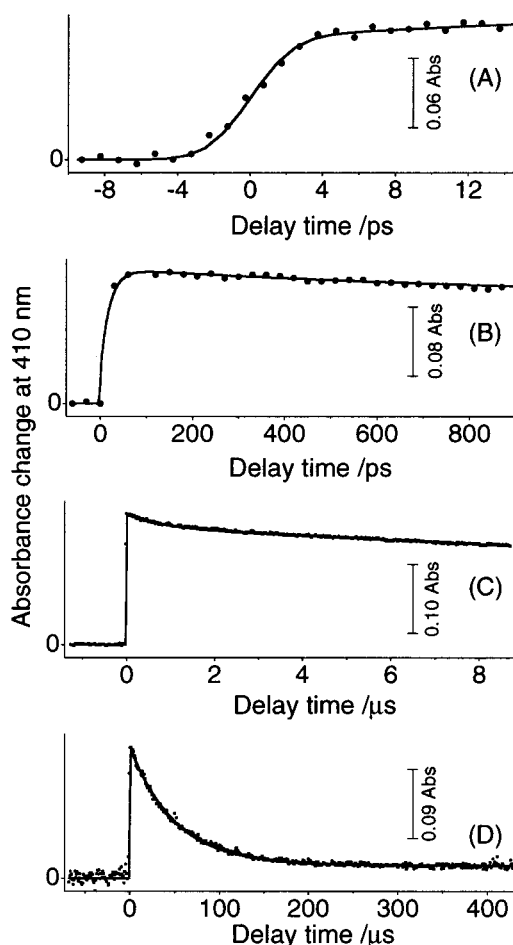


**Figure 3.** Time-resolved absorption signals probed at 410 nm for 2,4-Ph<sub>2</sub>BP in cyclohexane in various time regions. Dots show observed data; solid curves are best-fits simulated to the experimental points by convolution of the instrumental function with rise ( $\tau_1$ ) and/or decay ( $\tau_2$  and  $\tau_3$ ) exponential functions. (A) Pumped at 295 nm;  $\tau_1$ , 20 ps;  $\tau_2$ , 800 ps. (B) Pumped at 295 nm;  $\tau_1$ , 20 ps;  $\tau_2$ , 800 ps;  $\tau_3$ , 730 ns. (C) Pumped at 308 nm;  $\tau_2$ , 730 ns;  $\tau_3$ , 48  $\mu$ s. (D) Pumped at 308 nm;  $\tau_2$ , 48  $\mu$ s;  $\tau_3$ , >1 ms.

at 10 ps delay time changes to a sharp one at 80 ps. However, on excitation at 266 nm, the spectrum seems to change in a

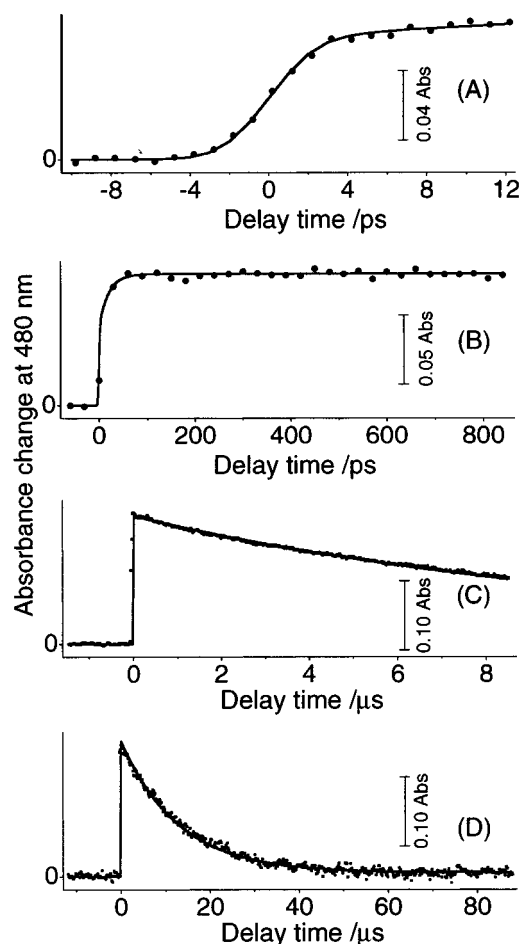


**Figure 4.** Time-resolved absorption signals probed at 470 nm for 2,2,4-Ph<sub>3</sub>BP in cyclohexane in various time regions. Dots show observed data; solid curves are best-fits simulated to the experimental points by convolution of the instrumental function with rise ( $\tau_1$ ) and/or decay ( $\tau_2$  and  $\tau_3$ ) exponential functions. (A) Pumped at 295 nm;  $\tau_1$ , 20 ps;  $\tau_2$ , 12  $\mu$ s. (B) Pumped at 295 nm;  $\tau_1$ , 20 ps;  $\tau_2$ , 12  $\mu$ s. (C) Pumped at 308 nm;  $\tau_2$ , 12  $\mu$ s;  $\tau_3$ , > 1 ms. (D) Pumped at 308 nm;  $\tau_2$ , 12  $\mu$ s;  $\tau_3$ , > 1 ms.

slight different way as shown in Figure 2B. On 295 nm excitation the spectrum around 425 nm decreases in intensity in this time range, but on 266 nm excitation the spectrum remains almost unchanged; the absorbance increments around 410 and 460 nm are smaller on 295 nm excitation, but larger on 266 nm excitation. Both the features of the spectra at 80 ps delay time are similar to those of the spectra observed with a nanosecond delay time in the region of 400–470 nm (Figure 1A).

Figures 3 and 4 show the time developments of the spectra monitored at 410 and 470 nm for 2,4-Ph<sub>2</sub>BP and 2,2,4-Ph<sub>3</sub>BP, respectively. All the observed time-resolved curves can be satisfactorily reproduced by the convolution of the instrument response function with rise and/or decay exponential functions. In the picosecond regions, the rise times of the induced absorption from both 2,4-Ph<sub>2</sub>BP and 2,2,4-Ph<sub>3</sub>BP are determined by the instrumental-limited rise component having a lifetime longer than hundreds of picoseconds and the small amplitude of the slower rise component with a rise constant of 20 ps. The ratio of the amplitude of the slow component to that of the very fast component is 0.22 for 2,4-Ph<sub>2</sub>BP (Figure 3A) and 0.25 for 2,2,4-Ph<sub>3</sub>BP (Figure 4A). The slower rise component arises from the spectral change occurring in tens of picoseconds as shown in Figure 2. The instrumental-limited rise indicates that the generation of the observed species is much faster than the

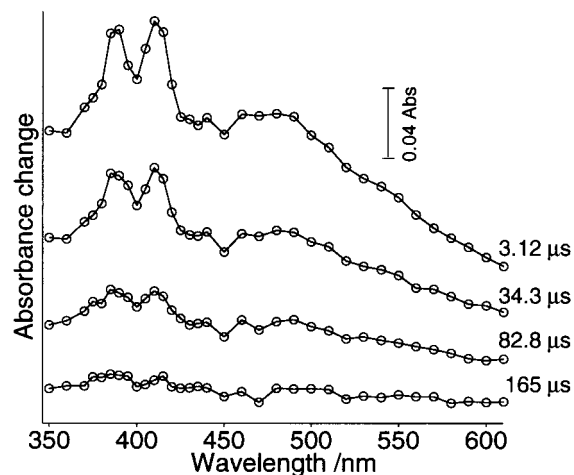


**Figure 5.** Time-resolved absorption spectra of 2,4-Ph<sub>2</sub>BP excited at 308 nm in cyclohexane in the microsecond time range. The delay time is given on the right of each spectrum.

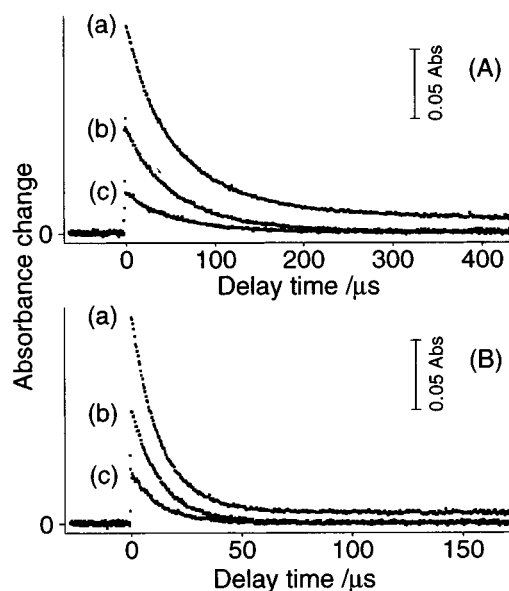


**Figure 6.** Pump-laser power dependence of time-resolved absorption signals for (A) 2,4-Ph<sub>2</sub>BP and (B) 2,2,4-Ph<sub>3</sub>BP in cyclohexane in the subnanoseconds to submillisecond time range. The approximate values of pump-laser power density are (a) 160 mJ cm<sup>-2</sup>, (b) 73 mJ cm<sup>-2</sup>, (c) 24 mJ cm<sup>-2</sup>. (A) pump, 308 nm; probe, 410 nm. (B) pump, 308 nm; probe, 470 nm.

temporal resolution of the present experimental system ( $\approx 2$  ps). The rise times are not affected by monitoring wavelength and by light polarization within the experimental accuracy. Several decay components are observed in the time range of subnanoseconds to submilliseconds, although the change in the spectral profile with the delay time is not observed clearly (Figures 1A and 5). For 2,4-Ph<sub>2</sub>BP, four components are observed with decay time constants of (1) several hundreds ps, (2) 730 ns, (3) 48  $\mu$ s, and (4) > 1 ms, and for 2,2,4-Ph<sub>3</sub>BP, two components with decay time constants of (1) 12  $\mu$ s and (2) > 1 ms. The components with lifetimes of 48  $\mu$ s for 2,4-Ph<sub>2</sub>BP and 12  $\mu$ s for 2,2,4-Ph<sub>3</sub>BP seem to be the major species induced by the UV irradiation (Figures 3D and 4D).

Figure 6 shows the pump-laser power dependence of the time-resolved absorption of 2,4-Ph<sub>2</sub>BP and 2,2,4-Ph<sub>3</sub>BP in the time regions of subnanoseconds to submilliseconds. The yields of the major components with lifetimes of 48  $\mu$ s for 2,4-Ph<sub>2</sub>BP and 12  $\mu$ s for 2,2,4-Ph<sub>3</sub>BP are linearly dependent on the pump-laser power, while those of the minor components with longer



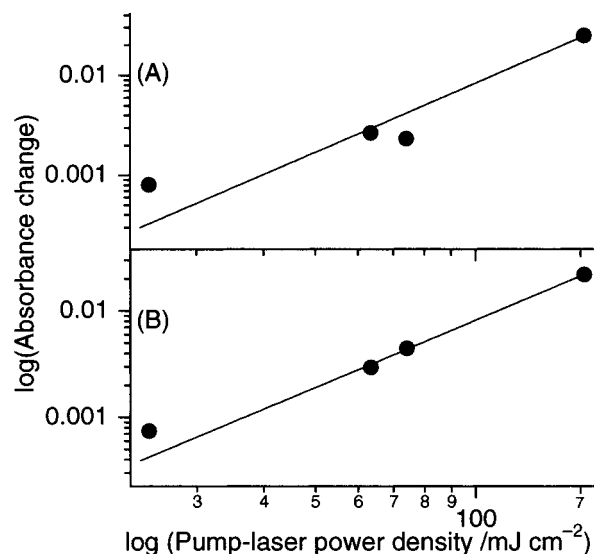


**Figure 7.** Plot of the transient absorption signals for (A) 2,4-Ph<sub>2</sub>BP and (B) 2,2,4-Ph<sub>3</sub>BP in cyclohexane in the submillisecond time range against the pump-laser power density on a log–log scale. (A) pump, 308 nm; probe, 410 nm; delay time, 250  $\mu$ s. (B) pump, 308 nm; probe, 470 nm; delay time 100  $\mu$ s. The lines are best-fits to the observed data. The slopes of the fitted lines are (A) 2.3 and (B) 2.1.

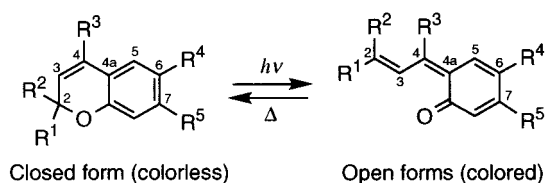
lifetimes ( $>1$  ms) increase in the approximately second order of the pump-laser power as shown in Figure 7. This result indicates that the major components are produced through a one-photon process whereas the minor long-lived components are produced through a two-photon process within a nanosecond pump-laser pulse.

**3.2. Effects of Substituents on Photochromism of Benzopyrans.** The wavelengths of absorption maxima of the closed and open forms are summarized in Table 1. Although no remarkable differences are observed in the two absorption maxima of the closed forms, the absorption spectra of the open forms can be classified into two groups: one that shows both the A and B bands such as 2,4-Ph<sub>2</sub>BP (Figure 1A), and the other that shows only the B band such as 2,2,4-Ph<sub>3</sub>BP (Figure 1B). The lifetimes of the major open forms at 298 K are also listed in Table 1, ranging in the wide time region; for example, the major component of 2,2,4-Ph<sub>3</sub>BP has a lifetime of 12  $\mu$ s; however, that of 2,2-Ph<sub>2</sub>BP has a lifetime longer than 1 ms. For 4-MeBP, 4-PhBP, 4-Me-2-PhBP, 2,4-Ph<sub>2</sub>BP, 4-Me-2,2-Ph<sub>2</sub>BP, and 2,2,4-Ph<sub>3</sub>BP, the activation parameters for disappearance of the major open forms are determined from the temperature dependence of their lifetimes in the region of 293–313 K (Table 1).

## 4. Discussion

**4.1. Mechanism of the C–O Bond Cleavage of 2,4-Ph<sub>2</sub>BP and 2,2,4-Ph<sub>3</sub>BP.** For both benzopyrans, 2,4-Ph<sub>2</sub>BP and 2,2,4-Ph<sub>3</sub>BP, the spectral rises are found to be faster than the instrumental detection limit ( $\approx 2$  ps), and the spectral profiles are similar to those of the open forms observed in the time regions of subnanoseconds to submilliseconds. These results indicate that the ring opening of the closed forms occurs within 2 ps, producing vibrationally excited open forms in the ground electronic state ( $S_0$ ). These observations are in agreement with the behavior of spiropyrans and their analogues reported so far;<sup>5,7,10,11,13,14,18,19</sup> the C–O bond of a spiropyran was shown to break in less than 100 fs to form a metastable species by means of time-resolved absorption spectroscopy.<sup>14</sup> For a spirooxazine the time constants for the C–O cleavage and the relaxation

## SCHEME 1



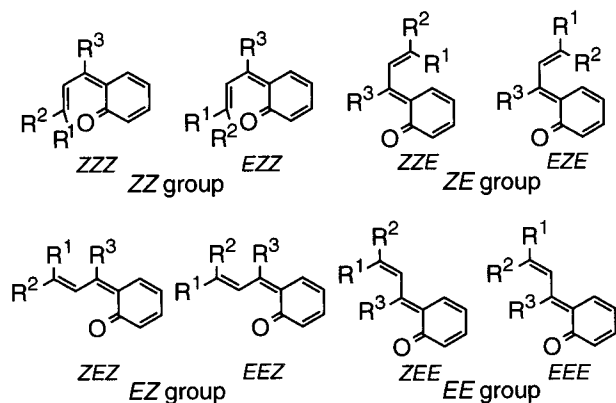
from a transition state to a metastable merocyanine were estimated to be approximately 700 and 470 fs, respectively.<sup>13</sup>

The fast rise is followed by a change with a time constant of about 20 ps. In this time region, a broad spectrum changes in profile to a sharp one, as seen in Figure 2. Immediately after the ring-opening reaction, vibrationally excited open forms in the  $S_0$  state should be generated because a large amount of excess vibrational energy [in this case, difference between electronic energies of the photoexcited closed form and the  $S_0$  state of the open forms] is expected. A relaxation process from vibrationally excited states to a thermodynamically favorable state may be hence observed spectroscopically. Generally speaking, it takes several to tens of picoseconds for vibrationally excited large molecules to reach a thermal equilibrium with surrounding solvent molecules, during which the spectral profile generally changes from a broad one to a sharp one.<sup>47,48</sup> Thus we may assign the spectral change in tens of picoseconds to the vibrational relaxation of the  $S_0$  open forms toward a thermal equilibrium with solvents.

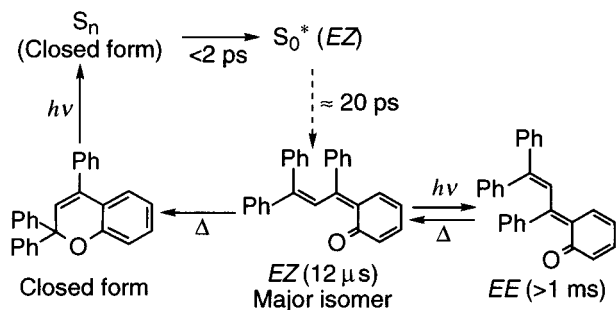
The vibrational relaxation behavior in the  $S_0$  open forms seems to depend on the pump wavelength as in Figure 2A,B. This means that the amount of the excess energy deposited in the  $S_0$  open forms depends on the pump-wavelength used to excite the  $S_0$  closed form. If the ring opening takes place from the lowest excited singlet state ( $S_1$ ) of the closed molecules after they reach a thermal equilibrium with surrounding solvent molecules through dissipation of the excess energy to solvents, the  $S_0$  open form would be formed with the same excess vibrational energy and the spectral change would be independent of the pump wavelength, 295 or 266 nm. Therefore, the pump-wavelength dependence of the spectral change suggests that the C–O cleavage does not occur from the  $S_1$  state of the closed form in a thermal equilibrium with solvent molecules. The two pump wavelengths (266 and 295 nm) may excite the different optical transitions of the closed form as listed in Table 1. The 266 nm pump photon creates a higher electronically excited ( $S_n$ ) state of the closed form, which should very rapidly relax to the vibrationally excited  $S_1$  closed form through internal conversion. As mentioned above, the ring opening of the closed form occurs within 2 ps and the C–O cleavage does not occur from the thermal equilibrium in the  $S_1$  closed form. Thus the  $S_n \rightarrow S_1$  internal conversion may compete with the ultrafast C–O bond cleavage.

**4.2. Structures and Dynamic Behavior of the Open Forms of 2,4-Ph<sub>2</sub>BP and 2,2,4-Ph<sub>3</sub>BP.** The decay components following vibrational relaxation exhibit almost the same spectral profiles within our experimental uncertainty (Figures 1 and 5); they are distinguished only by the decay time constants. Thus the components can be assigned to geometrical isomers of the open forms, and the difference in lifetime reflects the difference in the rate of the thermal reversion to the closed form. The open forms of benzopyrans consist of eight isomers with respect to two double bonds and one single bond as depicted in Scheme 2. The structures of the isomers are expressed by the geometries around the C<sub>2</sub>–C<sub>3</sub>, C<sub>3</sub>–C<sub>4</sub>, and C<sub>4</sub>–C<sub>4a</sub> bonds of benzopyrans; as an example, ZEE for an isomer with Z, E, and E geometries

## SCHEME 2



## SCHEME 3



around the  $C_2-C_3$ ,  $C_3-C_4$ , and  $C_4-C_{4a}$  bonds. The eight isomers can be classified into four groups, ZZ, EZ, ZE, and EE on the geometries around the  $C_3-C_4$  and  $C_4-C_{4a}$  bonds. In this manner, the two isomers in a group can be distinguished by different substituents,  $R^1$  and  $R^2$ , at the 2-position; for  $R^1 = R^2$ , the two isomers are reduced to an identical structure, and the resulting four isomers are expressed as ZZ, EZ, ZE, and EE.

Recently, Delbaere et al. have studied the photochromic behavior of 3,3-diphenyl-3H-naphtho[2,1-b]pyran, which corresponds to the case of  $R^1 = R^2$ , and identified the structures of the open forms with lifetimes of seconds to minutes by NMR.<sup>36</sup> Among four possible isomers of this naphthopyran molecule, two isomers ZZ and ZE with the Z geometry at the  $C_3-C_4$  single bond were discarded because of a large steric hindrance between the 2-phenyl group and the conjugate enone skeleton. The observed two components, a short-lived species with a lifetime of 9 s and a long-lived species with a lifetime of 2000 s, were identified as EZ and EE, respectively. It was also revealed that the photocleavage of the C–O bond yielded the two open forms in significantly different amounts, EZ as a major component and EE as a minor one.

In the case of 2,2,4-Ph<sub>3</sub>BP ( $R^1 = R^2 = R^3 = \text{Ph}$  in Scheme 2), the situation is very similar to the above naphthopyran molecule; the sterically unfavorable ZZ and ZE can be discarded. Hence, from comparison with the naphthopyran results, the major component with a lifetime of 12  $\mu\text{s}$  in Figure 4C is identified as EZ, and the remaining minor long-lived component with a lifetime longer than 1 ms is attributable to EE. The large difference in lifetime is rationalized in terms of the extent of structural change in reversion to the original closed form. The EZ isomer can easily revert to the closed form by the single-bond rotation, whereas EE needs the double-bond rotation in addition to the single-bond rotation. The obtained photochromic processes of 2,2,4-Ph<sub>3</sub>BP are depicted in Scheme 3.

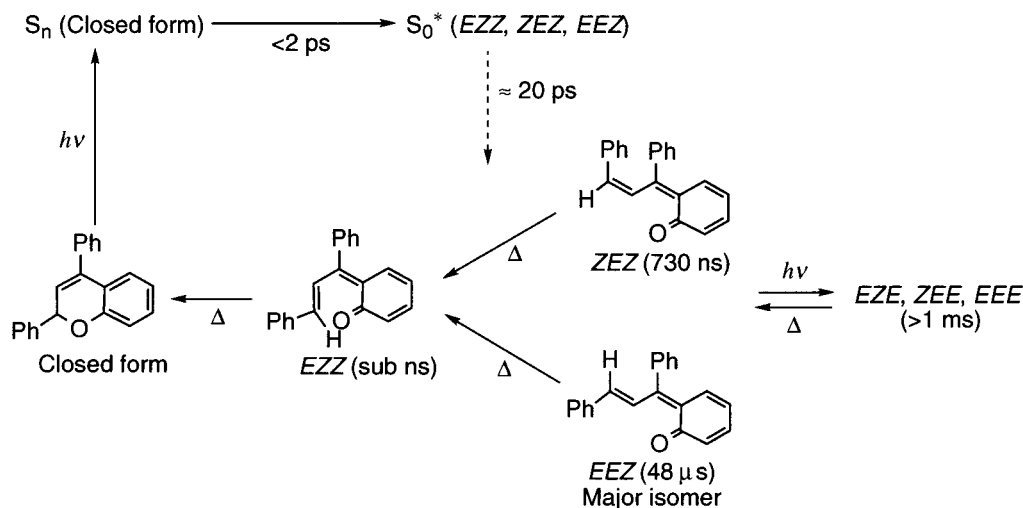
In the case of 2,4-Ph<sub>2</sub>BP ( $R^1 = R^3 = \text{Ph}$ ,  $R^2 = \text{H}$  in Scheme

2), the eight open forms are formed on photocleavage of the C–O bond. However, ZZZ and ZZE are hardly stabilized and can be discarded, since they suffer from a large steric hindrance between the 2-phenyl group and the conjugate enone skeleton. Among the remaining six isomers, EZE, ZEE, and EEE need the  $C_4-C_{4a}$  double-bond rotation on reverting to the closed form, as was discussed for EEs in 2,2,4-Ph<sub>3</sub>BP and the naphthopyran. The steric hindrance in ZEE of 2,4-Ph<sub>2</sub>BP is similar to that in EE of 2,2,4-Ph<sub>3</sub>BP, since both benzopyrans have the phenyl groups at the 2- and 4-positions at the side of the carbonyl oxygen atom. This suggests that the lifetime of ZEE may be comparable to that of EE of 2,2,4-Ph<sub>2</sub>BP. The EZE and EEE isomers, which have no steric interaction between the phenyl groups, are considered to be more stable than ZEE. From these considerations, EZE, ZEE, and EEE can be assigned to the residual components with lifetimes longer than 1 ms in Figure 3D.

The other three decay components are attributable to EZZ, ZEZ, and EEZ. Among those three isomers, the EZZ isomer can most easily revert to the closed form, and can be regarded as the most unstable species from comparison with the results of hexatriene isomers.<sup>49–52</sup> Thus, the EZZ isomer is tentatively assigned to the short-lived component with a lifetime of several hundreds of picoseconds. This assignment is consistent with the lack of a component with a lifetime of hundreds of picoseconds in the spectrum of 2,2,4-Ph<sub>3</sub>BP, where s-cis conformers are discarded on the large steric hindrance. Immediately after photocleavage of 1,3-cyclohexadienes, the time constants for formation of an s-trans conformer from an s-cis one have been reported to be several picoseconds.<sup>49–52</sup> As for previtamin D generated from the ring opening of 7-dehydrocholesterol, the s-cis to s-trans isomerization has been shown to occur with a time constant of 125 ps.<sup>53</sup> The lifetime assigned to the present EZZ isomer is longer than those for all-cis conformers of trienes reported so far.<sup>49–53</sup> This might be due to hydrogen bonding between the carbonyl group and the olefinic hydrogen in the present isomer.<sup>16</sup> The ring closure is a most plausible process for EZZ, though the isomerization to EZE or EEZ is not completely excluded. The ZEZ and EEZ isomers can revert to the closed form through a single-bond rotation; however, the steric hindrance between the phenyl groups at the 2- and 4-positions is larger in ZEZ than in EEZ. Therefore, the ZEZ isomer is considered to be faster in reversion and is assigned to the 730 ns component, and thus, the EEZ isomer to the 48  $\mu\text{s}$  component. The photochromic processes of 2,4-Ph<sub>2</sub>BP obtained in this study are depicted in Scheme 4.

As shown in Figures 6 and 7, the nanosecond pump-laser power dependence of the induced absorption signals indicates that the short-lived major components with a lifetime of tens of microseconds are produced by a one-photon process, whereas the long-lived minor components are formed through a two-photon process within a pump-laser pulse with 20 ns duration. Since the photocleavage of the C–O bond takes place within 2 ps after photoexcitation, the yield of the further excitation of the photoexcited closed form should be very small. Furthermore, no long-lived components were observed by the picosecond pump-laser pulse with a power density of 180  $\text{mJ cm}^{-2}$ , which is higher than those used in the measurements of nanosecond pump-laser power dependence. Therefore, it is concluded that the long-lived open isomers are formed from photoexcitation of the short-lived open isomers, but not from the closed form. In other words, the C–O photocleavage gives at first only the open forms which are revertible to the closed form by a single-bond rotation, and their photoisomerization leads to other open

## SCHEME 4



forms which need a double-bond rotation for reversion to the closed form. Since such a two-step two-photon behavior has also been observed very recently in the photochromism of 1H-benzopyran derivatives.<sup>54</sup> It may be said that the concept of two-step two-photon photochromism generating long-lived isomers applies to other photochromic systems.

The isomers are formed in very much different yields from photocleavage of 2,4-Ph<sub>2</sub>BP and 2,2,4-Ph<sub>3</sub>BP; the conformers which can revert to the closed form by a single-bond ( $C_3-C_4$ ) rotation, such as EZ in 2,2,4-Ph<sub>3</sub>BP and EEZ in 2,4-Ph<sub>2</sub>BP, are produced in a larger amount than those which need a double-bond ( $C_4-C_{4a}$ ) rotation for reverting to the closed form, such as EE in 2,2,4-Ph<sub>3</sub>BP and EZE in 2,4-Ph<sub>2</sub>BP. This difference may be ascribed to the difference between the one-photon and two-photon photoisomerization processes. In spiroopyran systems it has been proposed that thermal isomerization of the primary ring-opening product, the internal temperature of which is very high because of a large amount of excess vibrational energy generated via the C—O cleavage, is responsible for a distribution of merocyanines.<sup>10</sup> The present study suggests that the photoisomerization of the open forms also plays a significant role in the isomer distribution in some cases.

**4.3. Effects of Substituents on Photochromism of Benzopyrans.** As mentioned in Subsection 3.1, the benzopyrans are classified into two classes with respect to the spectrum of the open forms. Among those with a phenyl group at the 2-position ( $R^1$ ,  $R^2$  in Table 1), 2-PhBP, 4-Me-2-PhBP, 2,4-Ph<sub>2</sub>BP, and 2,2-Ph<sub>2</sub>BP show the structured A bands; however, no A band is observed for those with a sterically crowded structure, such as 4-Me-2,2-Ph<sub>2</sub>BP and 2,2,4-Ph<sub>3</sub>BP. The B band tends to be shifted with increasing the number of phenyl substituents; for example, the band maxima appear at 430, 445, 485, and 490 nm for BP, 2-PhBP, 2,2-Ph<sub>2</sub>BP, and 2,2,4-Ph<sub>3</sub>BP, respectively. Thus the B band is assigned to the conjugate systems of enones, which is in agreement with the theoretical calculations using an LCAO-MO-SCF-CI procedure.<sup>23</sup> The origin of the A band cannot be assigned in the present study, although it is noted that the spectra at delay time 82.8 and 165  $\mu$ s in Figure 5, which are considered to mainly arise from the double-bond rotated open forms of 2,4-Ph<sub>2</sub>BP, also exhibit the structured A band around 400 nm.

Disappearance of the major components observed in the nanosecond time-resolved absorption in Figures 3 and 4 can be identified to a thermal ring closure giving the original molecules. According to the discussion of 2,4-Ph<sub>2</sub>BP and 2,2,4-Ph<sub>3</sub>BP, the

major components are assigned to be the isomers which can revert to the closed form by a single-bond rotation: EEZ for 2-PhBP, 4-Me-2-PhBP, and EZ for BP, 4-MeBP, 4-PhBP, 2,2-Ph<sub>2</sub>BP, 4-Me-2,2-Ph<sub>2</sub>BP, and 2,2-Me<sub>2</sub>BPs. The preexponential factors ( $\log(A/s^{-1}) = 10.0-10.9$ ) for the major components of some benzopyrans (Table 1) indicate a significant loss of freedom ( $\Delta S^\ddagger_{\text{eff}} = -(45-60) \text{ J K}^{-1} \text{ mol}^{-1}$ ) in the decay process, reflecting the recyclization into the original closed form.

The lifetimes of the major components of the open forms at 298 K are dependent on the molecular structure. The benzopyrans bearing no substituent at the 4-position ( $R^3$  in Table 1), such as BP, 2-PhBP, 2,2-Ph<sub>2</sub>BP, and 2,2-Me<sub>2</sub>BPs, show a lifetime longer than 1 ms. On the contrary, the lifetimes of those with a substituent at the 4-position, such as 4-MeBP, 4-PhBP, 4-Me-2-PhBP, 2,4-Ph<sub>2</sub>BP, 4-Me-2,2-Ph<sub>2</sub>BP, and 2,2,4-Ph<sub>3</sub>BP, are in the order of microseconds. The size of the 4-substituents also affects the lifetimes of the main components: for 2,2-Ph<sub>2</sub>BP, 4-Me-2,2-Ph<sub>2</sub>BP, and 2,2,4-Ph<sub>3</sub>BP, which have a substituent of H, Me, and Ph, respectively, the lifetimes are >1 ms, 36  $\mu$ s, and 12  $\mu$ s. For the 2-substituents, increase in the number of the phenyl groups reduces the lifetime as seen for 4-PhBP (194  $\mu$ s), 2,4-Ph<sub>2</sub>BP (48  $\mu$ s), and 2,2,4-Ph<sub>3</sub>BP (12  $\mu$ s). Consequently, the rate for the ring closure depends on the structure; in particular, introduction of a substituent in the 4-position brings about steric hindrance against the 2-substituent to accelerate the ring closure involving a single-bond rotation.

## 5. Conclusion

The ring opening of benzopyrans, 2,4-Ph<sub>2</sub>BP and 2,2,4-Ph<sub>3</sub>BP, is completed within 2 ps, producing vibrationally excited open forms in the  $S_0$  state, which relax to thermal equilibria with a time constant of  $\approx 20$  ps. In 2,2,4-Ph<sub>3</sub>BP, two decay components are detected; the major component is short-lived and identified as the EZ isomer, which can revert to the closed form by the single-bond rotation. The minor long-lived component is assigned to the EE isomer; its reversion to the closed form needs the double-bond rotation in addition to the single-bond rotation. In 2,4-Ph<sub>2</sub>BP, among the observed four components, the most short-lived one is assigned to EZZ, which can most easily revert to the closed form. The long-lived components with lifetimes longer than 1 ms are assigned to EZE, ZEE, and EEE, all of which need the double-bond rotation to revert to the closed form. The ZEZ and EEZ isomers revert to the closed form through the single-bond rotation; however, the extent of



steric hindrance affects their reversion rates, faster for ZEZ and slower for EEZ.

The photocleavage of 2,4-Ph<sub>2</sub>BP and 2,2,4-Ph<sub>3</sub>BP gives at first only the open forms revertible to the closed form by the single-bond rotation, and they are photochemically isomerized, by a second photon within a nanosecond laser pulse, to the open isomers which need the double-bond rotation to revert to the closed form. Steric hindrance due to the size of a substituent at the 4-position and to the number of phenyl groups at the 2-position affects the rate of thermal reversion to the closed form.

## References and Notes

- (1) *Photochromism: Molecules and Systems*; Studies in Organic Chemistry 40; Dürr, H., Bouas-Laurent, H., Eds.; Elsevier: Amsterdam, 1990.
- (2) *Organic Photochromic and Thermochromic Compounds*; Crano, J. C., Guglielmetti, R. J., Eds.; Plenum Press: New York, 1999; Vols. 1 and 2.
- (3) Ward, M. D. *Chem. Ind.* **1997**, 640.
- (4) Willner, I. *Acc. Chem. Res.* **1997**, 30, 347.
- (5) Krysanov, S. A.; Alfimov, M. V. *Chem. Phys. Lett.* **1982**, 91, 77.
- (6) Takahashi, H.; Yoda, K.; Isaka, H.; Ohzeki, T.; Sakaino, Y. *Chem. Phys. Lett.* **1987**, 140, 90.
- (7) Schneider, S.; Mindl, A.; Elfinger, G.; Melzig, M. *Ber. Bunsen-Ges. Phys. Chem.* **1987**, 91, 1222.
- (8) Schneider, S.; Baumann, F.; Klüter, U.; Melzig, M. *Ber. Bunsen-Ges. Phys. Chem.* **1987**, 91, 1225.
- (9) Kellmann, A.; Tfibel, F.; Dubest, R.; Levoir, P.; Aubard, J.; Pottier, E.; Guglielmetti, R. *J. Photochem. Photobiol. A: Chem.* **1989**, 49, 63.
- (10) Ernsting, N. P.; Arthen-Engeland, T. *J. Phys. Chem.* **1991**, 95, 5502.
- (11) Aramaki, S.; Atkinson, G. H. *J. Am. Chem. Soc.* **1992**, 114, 438.
- (12) Bohne, C.; Fan, M. G.; Li, Z. J.; Liang, Y. C.; Luszyk, J.; Scaiano, J. C. *J. Photochem. Photobiol. A: Chem.* **1992**, 66, 79.
- (13) Tamai, N.; Masuhara, H. *Chem. Phys. Lett.* **1992**, 191, 189.
- (14) Zhang, J. Z.; Schwartz, B. J.; King, J. C.; Harris, C. B. *J. Am. Chem. Soc.* **1992**, 114, 10921.
- (15) Salemi-Delvaux, C.; Luccioni-Houze, B.; Baillet, G.; Giusti, G.; Guglielmetti, R. *J. Photochem. Photobiol. A: Chem.* **1995**, 91, 223.
- (16) Day, P. N.; Wang, Z.; Pachter, R. *J. Phys. Chem.* **1995**, 99, 9730.
- (17) Pimienta, V.; Lavabre, D.; Levy, G.; Samat, A.; Guglielmetti, R.; Micheau, J. C. *J. Phys. Chem.* **1996**, 100, 4485.
- (18) Wilkinson, F.; Worrall, D. R.; Hobley, J.; Jansen, L.; Williams, S. L.; Langley, A. J.; Matousek, P. *J. Chem. Soc., Faraday Trans.* **1996**, 92, 1331.
- (19) Tamai, N.; Miyasaka, H. *Chem. Rev.* **2000**, 100, 1875.
- (20) Becker, R. S.; Michl, J. *J. Am. Chem. Soc.* **1966**, 88, 5931.
- (21) Becker, R. S.; Dolan, E.; Balke, D. E. *J. Chem. Phys.* **1969**, 50, 239.
- (22) Kolc, J.; Becker, R. S. *Photochem. Photobiol.* **1970**, 12, 383.
- (23) Edwards, L.; Kolc, J.; Becker, R. S. *Photochem. Photobiol.* **1971**, 13, 423.
- (24) Padwa, A.; Au, A.; Lee, G. A.; Owens, W. *J. Org. Chem.* **1975**, 40, 1142.
- (25) Zerbetto, F.; Monti, S.; Orlandi, G. *J. Chem. Soc., Faraday Trans. 2* **1984**, 80, 1513.
- (26) Lenoble, C.; Becker, R. S. *J. Photochem.* **1986**, 33, 187.
- (27) Van Gemert, B.; Bergomi, M.; Knowles, D. *Mol. Cryst. Liq. Cryst.* **1994**, 246, 67.
- (28) Pozzo, J.-L.; Samat, A.; Guglielmetti, R.; Lokshin, V.; Minkin, V. *Can. J. Chem.* **1996**, 74, 1649.
- (29) Aldoshin, S.; Chuev, I.; Utenyshev, A.; Filipenko, O.; Pozzo, J.-L.; Lokshin, V.; Guglielmetti, R. *Acta Crystallogr.* **1996**, C52, 1834.
- (30) Luccioni-Houze, B.; Campredon, M.; Guglielmetti, R.; Giusti, G. *Mol. Cryst. Liq. Cryst.* **1997**, 297, 161.
- (31) Pozzo, J.-L.; Samat, A.; Guglielmetti, R.; Dubest, R.; Aubard, J. *Helv. Chim. Acta* **1997**, 80, 725.
- (32) Celani, P.; Bernardi, F.; Olivucci, M.; Robb, M. A. *J. Am. Chem. Soc.* **1997**, 119, 10815.
- (33) Crano, J. C.; Flood, T.; Knowles, D.; Kumar, A.; Van Gemert, B. *Pure Appl. Chem.* **1996**, 68, 1395.
- (34) Luthern, J. *J. Mol. Cryst. Liq. Cryst.* **1997**, 297, 155.
- (35) Favaro, G.; Mazzucato, U.; Ottavi, G.; Becker, R. *Mol. Cryst. Liq. Cryst.* **1997**, 298, 137.
- (36) Delbaere, S.; Luccioni-Houze, B.; Bochu, C.; Teral, Y.; Campredon, M.; Vermeersch, G. *J. Chem. Soc., Perkin Trans. 2* **1998**, 1153.
- (37) Ottavi, G.; Favaro, G.; Malatesta, V. *J. Photochem. Photobiol. A: Chem.* **1998**, 115, 123.
- (38) Pozzo, J.-L.; Lokshin, V.; Samat, A.; Guglielmetti, R.; Dubest, R.; Aubard, J. *J. Photochem. Photobiol. A: Chem.* **1998**, 114, 185.
- (39) Van Gemert, B. In *Organic Photochromic and Thermochromic Compounds*; Crano, J. C., Guglielmetti, R. J., Eds.; Plenum Press: New York, 1999; Vol. 1, Chapter 3.
- (40) Sartori, G.; Casiraghi, G.; Bolzoni, L.; Casnati, G. *J. Org. Chem.* **1979**, 44, 803.
- (41) Kirkiacharian, B. S.; Danan, A.; Koutsourakis, P. G. *Synthesis* **1991**, 879.
- (42) Heilbron, I. M.; Hill, D. W. *J. Chem. Soc.* **1927**, 2005.
- (43) Woodruff, E. H. *Org. Synth., Coll. Vol. 3* **1955**, 581.
- (44) Subramanian, R. S.; Balasubramanian, K. K. *Tetrahedron Lett.* **1988**, 29, 6797.
- (45) Barnes, C. S.; Strong, M. I.; Occolowitz, J. L. *Tetrahedron* **1963**, 19, 839.
- (46) Freeman, J. P.; Hawthorne, M. F. *J. Am. Chem. Soc.* **1956**, 78, 3366.
- (47) Elsaesser, T.; Kaiser, W. *Annu. Rev. Phys. Chem.* **1991**, 42, 83.
- (48) Nakabayashi, T.; Okamoto, H.; Tasumi, M. *J. Phys. Chem. A* **1998**, 102, 9686.
- (49) Reid, P. J.; Doig, S. J.; Wickham, S. D.; Mathies, R. A. *J. Am. Chem. Soc.* **1993**, 115, 4754.
- (50) Reid, P. J.; Lawless, M. K.; Wickham, S. D.; Mathies, R. A. *J. Phys. Chem.* **1994**, 98, 5597.
- (51) Pullen, S.; Walker, L. A., II.; Donovan, B.; Sension, R. *J. Chem. Phys. Lett.* **1995**, 242, 415.
- (52) Lochbrunner, S.; Fuss, W.; Schmid, W. E.; Kompa, K.-L. *J. Phys. Chem. A* **1998**, 102, 9334.
- (53) Fuss, W.; Höfer, T.; Hering, P.; Kompa, K. L.; Lochbrunner, S.; Schikarski, T.; Schmid, W. E. *J. Phys. Chem.* **1996**, 100, 921.
- (54) Haba, E.; Segawa, K.; Sakuragi, H. *Mol. Cryst. Liq. Cryst.* in press.